



OPEN Future glacio-hydrological changes in the Andes: a focus on near-future projections up to 2050

Alexis Caro^{1,2}✉, Thomas Condom¹, Antoine Rabatel¹, Rodrigo Aguayo³ & Nicolas Champollion¹

Assessing future water contributions from glaciers is crucial for managing water resources, preventing disasters, and protecting ecosystems and communities. However, Andean glacier remains poorly understood because of missing regional and local research studies. We evaluated eight CMIP6 models

21st century in 778 Andean catchments (11°N–55°S), using the Open Global Glacier Model (OGGM) under two extreme climate change scenarios (SSP1-2.6 and 8.5). Projections for the mid-21st century show warming trends across the Andes, particularly in the Tropical Andes (+0.7 °C), while precipitation declines slightly in the Southern Andes (-1 to -3%).

with substantial decreases projected for the Tropical Andes (-43%) and Dry Andes (-37%) by 2030–2049. Notably, the Dry Andes, as evidenced by the simulations for the Atuel (-62%) and Tupungato (+32%) catchments in Argentina. More than 95% of Andean catchments are expected to reach peak water before 2030 (75th percentile

catchment scale, particularly in the Dry Andes of Chile and Argentina. It calls on these governments to and future water resources.

The water contribution from glaciers is crucial for downstream societies and ecosystems, particularly during dry seasons with prolonged months of no precipitation and during increasingly frequent dry years across the Andes^{1–3}. Over the past few decades, glacier runoff has increased by 12%, while the volume of glaciers has reduced by 8%⁴. Notably, in the Tropical and Dry Andes regions, some zones have seen the largest increases in glacier runoff, experiencing a rise of up to 73% between 2000 and 2009 and 2010–2019. However, the impacts of the glacier runoff on social-ecological systems remain unclear, potentially affecting water availability and water quality⁵.

In the Andes, most of the knowledge regarding future glacier changes is derived from global simulations (e.g., Marzeion et al.⁶, Radic and Hock⁷ and Huss and Hock⁸). Recent global studies^{9,10} stands out as it incorporates geodetic mass balance measurements obtained at the scale of individual glaciers by Hugonnet et al.¹¹ to calibrate the glacier mass balance during the historical period. It is important to note that these global-scale studies have not been specifically evaluated for the Andes, even though simulating current observations is a crucial prerequisite for predictive models¹². Glacier volume changes projected throughout the 21st century reported in the above mentioned studies show consistent results in the Tropical Andes, with an approximate loss of glacier mass of around $-97 \pm 4\%$ to $-99 \pm 3\%$ 2100 under the Representative Concentration Pathways 8.5 (RCP8.5) and Shared Socioeconomic Pathways 8.5 (SSP5-8.5) scenario based on the Coupled Model Intercomparison Project phase 5 (CMIP5) and phase 6 (CMIP6) models, respectively. However, in the Southern Andes, which encompasses the largest glacierized area, there is a wider range of mass loss estimates, ranging from $-44 \pm 14\%$ to $-74 \pm 27\%$ ^{9,10,13}. Even under the most optimistic scenarios (i.e. RCP2.6 and SSP1-2.6), the reduction in glacier volume remains significant. Furthermore, in a global study by Huss and Hock⁸ the estimated glacier runoff in 12 Andean catchments, which includes ice melt, snow melt and rainfall on glaciers, show an increase and subsequent reduction before 2050 in most of the catchments. After 2050, it is expected that this reduction will continue in all catchments except in the Santa Cruz catchment (49°S, Argentina).

In the Tropical Andes, Vuille et al.¹⁴ estimated that the Antizana Glacier (0°S, inner tropics) is more vulnerable to warming throughout the 21st century compared to Zongo Glacier (16°S, outer tropic). For Zongo Glacier,

¹Institut des Géosciences de l'Environnement, Univ. Grenoble Alpes, CNRS, IRD, INRAE, Grenoble-INP, Grenoble, France. ²Department of Civil Engineering, Universidad de La Frontera, Temuco, Chile. ³Department of Water and Climate, Vrije Universiteit Brussel, Brussels, Belgium. ✉email: alexis.caroparedes@gmail.com

projected volume losses range from $-40 \pm 7\%$ to $-89 \pm 4\%$ between 2010 and 2100 depending on the considered RCP¹⁵ and a discharge reduction in 2100 is estimated to 25% at the annual scale and to 57% during the dry season for RCP4.5¹⁶. In the Southern Andes, Ayala et al.² estimate glacier volume and glacier runoff changes under synthetic scenarios of committed ice loss, assuming a constant climate until the end of the century, indicating continued glacier shrinkage. The analysis projects an ice loss of 20% (relative to the volume in the year 2000) between the periods 1955–2016 and 2081–2100. However, the uncertainty of these glacier changes is significant due to the reliance on multiple linear regression analysis. In the Wet Andes, Scheiter et al.¹⁷ projected an ice volume loss between -56 and -97% in 2100 depending on the RCP for the Mocho Choshuenco glacier (40°S , Chile). Two other studies reported future glacier changes in the Patagonian icefields. In the Northern Patagonian Icefield (NPI) a strong increase in ablation is estimated from 2050 onward with a reduction of solid precipitation from 2080 onward due to higher temperatures, with uncertainties arising from future climate and ice dynamics¹⁸. Bravo et al.¹⁹ compared simulations for the period 2005–2050 with the historical period 1976–2005 and estimated a larger reduction in annual mass balance between -1.5 to -1.9 m w.e./yr for the NPI compared to the Southern Patagonian Icefield (SPI) (-1.1 to -1.5 m w.e./yr).

As glaciers continue to reduce under projected climate change scenarios, it becomes imperative to better forecast the timing of peak water (PW) - the period when glacier runoff increases before eventually declining - throughout the Andes taking into account regional peculiarities. This knowledge holds paramount importance as it enables stakeholders to anticipate when glacier contributions to river flows will decrease or even cease in the future. Because of that, the influence of uncertainties in future climate scenarios on future glacier changes has been a subject of investigation, as discussed by Marzeion et al.²⁰. Their study indicates that both at the global and regional scales, the relative uncertainty in future climate scenarios increases over the course of the 21st century. However, in contrast, the relative uncertainties related to the glacier model parameterization decrease over time. Furthermore, Hausfather et al.²¹ found that more than one-quarter of the models in the Coupled Model Intercomparison Project 6 (CMIP6)²² have higher variability in temperature compared to the CMIP5 models. This higher variability in temperature projections could introduce additional uncertainty in the estimates of future glacier changes. Similarly, Tokarska et al.²³ highlighted that certain CMIP6 models with high climate sensitivity (i.e. beyond the Fifth Assessment Report (AR5) likely range of 1.5 – 4.5 °C by the end of the 21st century) tend to overestimate historical warming trends. Consequently, this bias might lead to future warming projections being biased towards higher temperatures in these CMIP6 models. Conversely, CMIP6 models with climate sensitivity values within the likely range exhibit warming trends consistent with observations over the historical period, providing more reliable estimates for future climate scenarios and their impact on glaciers.

This study aims to address the lack of specific estimates regarding future glacier changes and their hydrological implications in the Andean glacierized catchments. For this we use a calibrated/validated version of the Open Global Glacier Model (OGGM²⁴) implemented across the Andes (11°N to 55°S) and feed it with a corrected version of TerraClimate dataset during the historical period 2000–2019⁴. The OGGM is an open-source continuously updated glaciological model. Using inputs like glacier outlines and digital elevation models, OGGM computes flowlines. With climate data and geodetic mass balance from Hugonnet et al.¹¹, a temperature-index model is calibrated to calculate the monthly mass balance. Based on mass-conservation, the model estimates ice flux at each glacier grid point, assuming a parabolic cross-section shape. Through the shallow ice approximation, OGGM calculates glacier thickness along flowlines and total glacier volume^{24,25}. As climate uncertainty plays a critical role in hydrological projections²⁶, the implementation of OGGM by Caro et al.⁴ used corrected climate variables and validated results across the Andes, marking the first study to calibrate OGGM with a local climate for the entire region. This calibration revealed a mean temperature bias ranging from 1.2 °C in the tropical Andes to 0.4 °C in the Wet Andes, highlighting the need for precise climate modeling in glaciological studies. Furthermore, a precipitation factor of up to 4 was necessary to accurately represent temperature variations with elevation and to effectively distinguish between solid and liquid precipitation. These findings were consistent with temperature-index factors and Glen's A inversion values across different glacier zones, with three tested catchments (16 , 33 and 47°S) confirming both previous findings and novel insights.

In the present study, we analyze historical (1990–2019) and short-term (2020–2049) climates, evaluating eight GCMs from CMIP6 across the Andes (11°N – 55°S). Using an ensemble of high-score GCMs (filtered ensemble), we examine future changes in glacier runoff simulations (including ice and snowmelt) across 778 Andean glacierized catchments. We compare the mean glacier runoff for 2030–2049 with the calibration period of the model (2000–2019). Additionally, we estimate peak water throughout the 21st century, with a focus on the first half. The discussion addresses uncertainties related to the simulated glacier evolution and compares these results with previous global peak water simulations estimated for some large Andean catchments.

Results

Analysis of past and future climate conditions in the Andes

Historical period (1990–2019)

This section analyzes the correlations and differences between downscaled Global Climate Models (GCMs) and corrected TerraClimate data (cTC) across the Andes region, focusing on a monthly and seasonal scale during the historical period (1990–2019) for 3,213 glaciers (covering $27,669$ km²). At the monthly time series scale, bias-corrected GCMs and cTC exhibit statistically significant correlations across all glaciers for temperature ($r=0.9$) and precipitation ($r=0.4$) (Figure S1E). However, the GCM monthly time series reveal temperature differences of 1.1 ± 0.1 °C (RMSE) and precipitation differences of 106 ± 68 mm (RMSE). Among the glaciological regions, the Dry and Wet Andes show the largest discrepancies in both temperature and precipitation, followed by the Tropical Andes (Figure S2). After applying bias correction to the GCMs, no differences are observed in the mean monthly values for either variable during the historical period, where the bias is effectively zero. At a seasonal scale, there are significant correlations for temperature and precipitation on a lower number of glaciers (close to

30%) during specific seasons (Table S1). For example, in the Tropical Andes, correlations are significant in JFM and AMJ for precipitation, and in OND for temperature. In the Dry Andes, a considerable number of glaciers show significant correlations in all seasons. Meanwhile, in the Wet Andes, significant correlations are observed in JFM and AMJ for temperature and during JAS and OND for precipitation.

Considering that the largest glacier mass loss occurs through the transition season (OND) in the Tropical Andes and during the summer season (JFM) in the Dry and Wet Andes, we scored the GCMs regarding their performance for temperature and precipitation in these seasons (see Figure S1A–D). In the Tropical Andes, the largest number of glaciers is better correlated with INM-CM5 for both climate variables, while GFDL and NorESM2 were for temperature, and FGOALS for precipitation. In the Dry Andes, no single model showed a high performance for both climate variables. However, CAMS and NorESM2 showed a high performance for temperature, while MPI and CESM2 were more accurate for precipitation. In the Wet Andes, the INM-CM4 model exhibits the highest correlations in temperature and precipitation across the majority of glaciers. Additionally, the GFDL, INM-CM4, FGOALS, and MPI models accurately reproduce precipitation patterns. Conversely, the INM-CM4 model is relevant for only a very small number of glaciers in the Tropical Andes and Dry Andes, and the MPI model was in the Tropical Andes and Wet Andes. Based on this correlation analysis, eight models are selected for the short-term future period modeling (2020–2049). These findings provide valuable insights into the GCMs' performance and allow considering the most relevant one to simulate the future glacier mass loss across the Andes.

Short-term future period (2020–2049)

We analyze the differences in mean temperature and precipitation during the periods 1990–2019 and 2020–2049 for each individual glacier considering the eight GCMs. The differences led us to define the likely ranges of climate change by glaciological region considering the percentiles 10 and 90. The objective is to identify the models that are outside the regional climate change likely ranges at the annual and seasonal scales, which are then considered as hot/cold and dry/wet models.

At an annual scale, both scenarios (SSP1-2.6 and SSP5-8.5) exhibit the most significant temperature increase in the Tropical Andes (median = 0.7 and 0.9 °C, respectively), followed by the Dry (median = 0.6 and 0.9 °C) and Wet Andes (median = 0.4 and 0.6 °C). Notably, SSP5-8.5 depicts a warmer outcome. In contrast, precipitation is projected to decrease in all glaciological regions and scenarios, except for the Tropical Andes under the SSP1-2.6 scenario (median = +0.6%). The Dry Andes show the most considerable precipitation reduction (median = -2.8 and -1.9%), trailed by the Wet Andes (median = -2.6 and -0.8%) and the Tropical Andes (median = -0.8). At a seasonal scale, the largest increase in median temperature is observed in the SSP5-8.5 scenario, particularly in the Tropical Andes (JAS = +1.1 °C), followed by the Dry (OND and JFM = +1.0 °C) and Wet Andes (JFM = +0.7 °C). Regarding precipitation changes, the Tropical Andes (JFM) are estimated to experience the most significant increase, while the Dry Andes show lower negative median total precipitation during OND. Detailed percentile values can be found in Table S2 and Fig. 1.

Temperature and precipitation play a crucial role in glacier mass loss during the transition (OND) and wet seasons (JFM) in the Tropical Andes. The largest glacier ablation occurs during the transition season⁵ and any delay in precipitation during the wet season can lead to a significant increase in ablation rates²⁷. In the Tropical Andes, the models project a median temperature increase in 0.7 °C (SSP1-2.6) and 0.9 °C (SSP5-8.5) during both seasons. Precipitation is expected to decrease during the transition season by -0.9 to -0.8% and increase during the wet season by 1.4 to 1.7%. Conversely, in the Southern Andes, glacier accumulation is concentrated in autumn/winter (AMJ and JAS), although significant precipitation also occurs in spring and summer in the Wet Andes (OND and JFM). During summer, the increased precipitation contributes to reducing the strong glacier ablation rates due to an increase in albedo. In the Dry Andes, models indicate a median temperature increase in 0.6 °C (SSP1-2.6) and 1 °C (SSP5-8.5) during spring and summer. However, scenarios differ significantly in terms of precipitation. Under the SSP5-8.5 scenario, median precipitation is projected to decrease by 8.8% during spring and remain unchanged during summer. On the other hand, the SSP1-2.6 scenario shows an increase in median precipitation during spring (1.2%) and a reduction during summer (-2.7%). As for the Wet Andes, both scenarios exhibit a reduction in median precipitation, with the largest impact observed during summer (precipitation reduction of -2.4 to -4.5%) compared to spring (precipitation reduction of -1.9 to -4%). Additionally, the median temperature increase is more significant in summer (temperature rise of 0.5–0.7 °C) than in spring (temperature rise of 0.4–0.5 °C). For detailed values, please refer to Table S2.

From the regional temperature and precipitation likely ranges (Fig. 1A–B for annual and Fig. 1C for seasonal), we identified hot/cold and dry/wet models. On an annual scale, for the Tropical Andes, GCMs' median values remain within likely ranges for both climate change scenarios. However, in the Dry Andes, FGOALS exhibits hot/dry characteristics and CAMS is a wet model. Moving to the Wet Andes, CESM2 and GFDL models are dry and cold, respectively, while FGOALS is a hot model. At the seasonal scale, FGOALS and CESM2 display mean values outside the likely ranges. Specifically, in the Tropical Andes, CESM2 is a hot model during (OND). In the Dry Andes, FGOALS (OND) and CESM2 (JFM) are hot models, whereas CAMS (OND) and FGOALS (JFM) are wet models. In the Wet Andes, the FGOALS model is hot/dry (OND).

In summary, considering the analysis performed in Sect. 2.1.2 and 2.2.2, we identified that the highest score GCMs were: CAMS, FGOALS, GFDL, INM-CM5, and NorESM2 in the Tropical Andes; GFDL, INM-CM5, MPI, and NorESM2 for the Dry Andes; CAMS, INM-CM4, and NorESM2 in the Wet Andes. In the following, we analyze changes in glacier runoff and PW considering both the filtered ensemble of GCMs (highest score GCMs) and the complete ensemble of all GCMs.

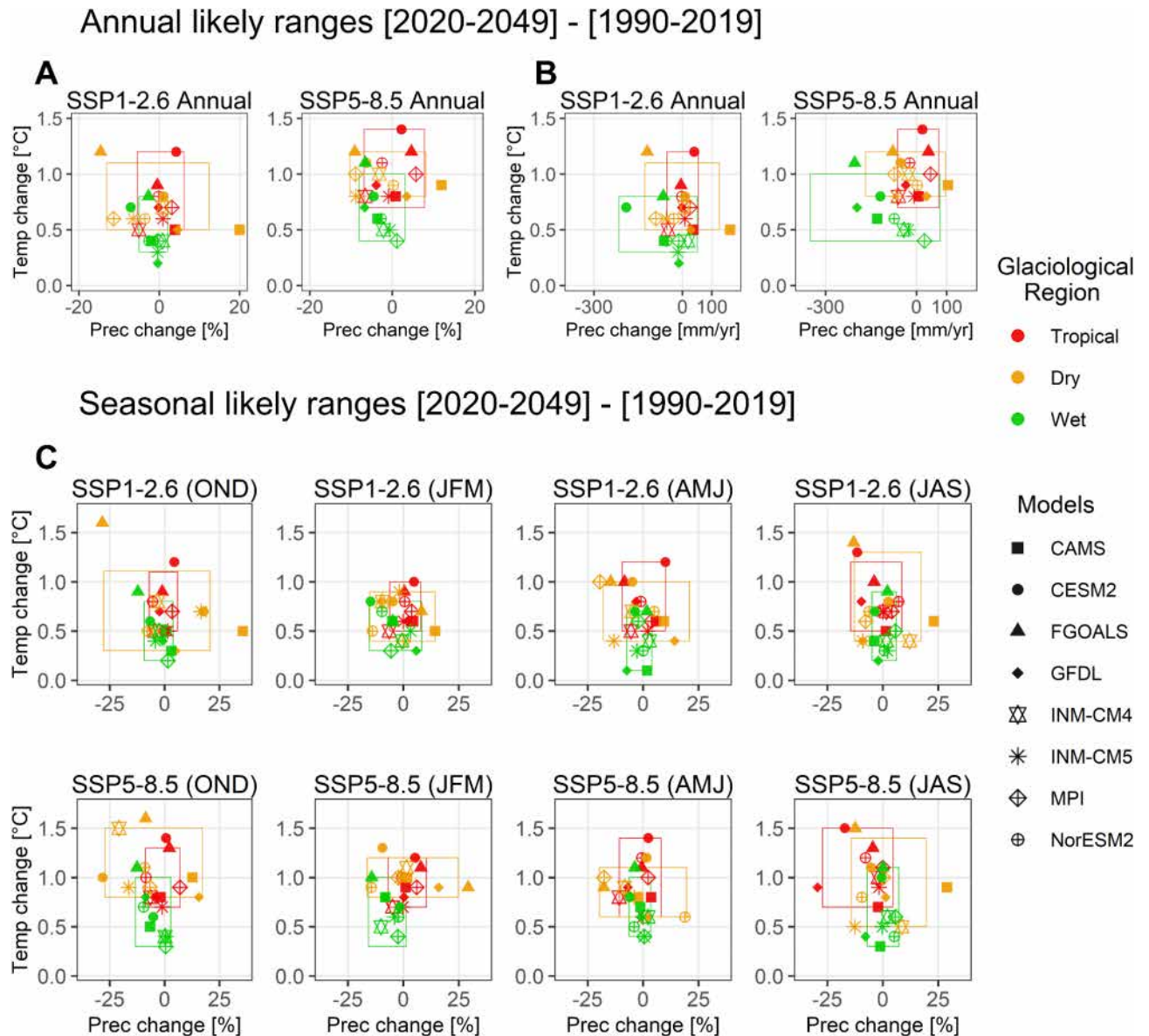


Fig. 1. Temperature and precipitation changes between the historical (1990–2019) and future periods (2020–2049) across the glaciological Andean regions in two climate change scenarios. Percentiles 10 and 90 (boxes, likely ranges) from mean differences in both periods are estimated considering all glaciers in the complete ensemble of GCMs. Annual climate change likely ranges are exhibited in terms of absolute (A) and relative values (B) for precipitation considering SSP1-2.6 and SSP5-8.5 scenarios. (C) show these differences by seasons considering both scenarios. Estimations are performed using 3,213 glaciers (27,668 km²) (TA = 598, DA = 370, WA = 2245). Models situated inside the boxes formed the filtered ensemble.

Future evolution of Andes glaciers

Future glacier runoff changes (2030–2049)

This section focuses on analyzing the mean annual changes in glacier runoff between two distinct periods: 2000–2019 and 2030–2049.

To estimate these changes, we use the filtered and complete ensembles of GCMs. The analysis is conducted at both the glaciological region and catchment scales, taking into account the cumulative volumes of glacier runoff by catchment. Although changes in glacier runoff were observed in both periods under the SSP5-8.5 scenario, the two ensembles showed similar differences at the Andean scale. The filtered ensemble indicated a reduction in runoff in 680 catchments, compared to 674 in the complete ensemble. Within the Dry Andes, the filtered ensemble revealed more catchments with reduced glacier runoff (74 catchments) than the complete ensemble (68 catchments). Notably, in the six catchments where the two ensembles do not agree, glacier runoff decreases by up to -6% in the filtered ensemble, while it increases by up to 8% in the complete ensemble. Furthermore, the median of the differences in mean glacier runoff during the period 2030–2049 is zero for both ensembles in the

Andes. However, these differences are significant at the regional and catchment scales. In the Dry Andes, the median difference between the two ensembles is 7%, while in certain catchments in the Wet and Dry Andes, the difference increases to 50% and 33%, respectively.

These differences, along with the better historical fit demonstrated by certain GCMs, led us to focus our analysis on the simulation results of the filtered ensemble. Changes in mean annual glacier runoff using the complete ensemble of GCMs can be found in Table S3 and Figure S3 in the Supplementary Information.

Figure 2 illustrates the mean annual changes in glacier runoff in absolute and relative terms, by comparing the historical and future periods for the 778 catchments analyzed in the Andes. Three distinct types of behavior in glacier runoff changes are observed across catchments for the SSP1-2.6 and SSP5-8.5 scenarios (Table S4). These behaviors include positive changes, negative changes, and catchments exhibiting positive changes under SSP5-8.5 and negative changes under SSP1-2.6. The largest volume changes in glacier runoff are consistently negative across all regions and time periods (2000–2019 and 2030–2049) for both scenarios. The Tropical Andes exhibit the most significant cumulative loss of glacier runoff in terms of percentage regarding the historical period, with a reduction of 43% ($-25.8 \text{ m}^3 \text{ s}^{-1}$ in SSP1-2.6). The Dry Andes follow, with a cumulative loss of 37% ($-14.4 \text{ m}^3 \text{ s}^{-1}$ in SSP1-2.6), and the Wet Andes, with a cumulative loss of 32% ($-177.2 \text{ m}^3 \text{ s}^{-1}$ in SSP1-2.6, cumulative loss of all glaciers in the region). However, a smaller number of catchments ($n=22$) show an increase in glacier runoff, mainly in the Dry Andes, experiencing a 38% increase ($+3.5 \text{ m}^3 \text{ s}^{-1}$ in SSP5-8.5). Some catchments show both increases or reductions in glacier runoff depending on the scenario. In the Dry Andes (Figure S4), these catchments show a 6% increase ($+1.1 \text{ m}^3 \text{ s}^{-1}$) in the SSP5-8.5 scenario and a 7% reduction ($-1.4 \text{ m}^3 \text{ s}^{-1}$) in the SSP1-2.6 scenario. Notably, the Olivares catchment and Cipreses catchment in Chile are among

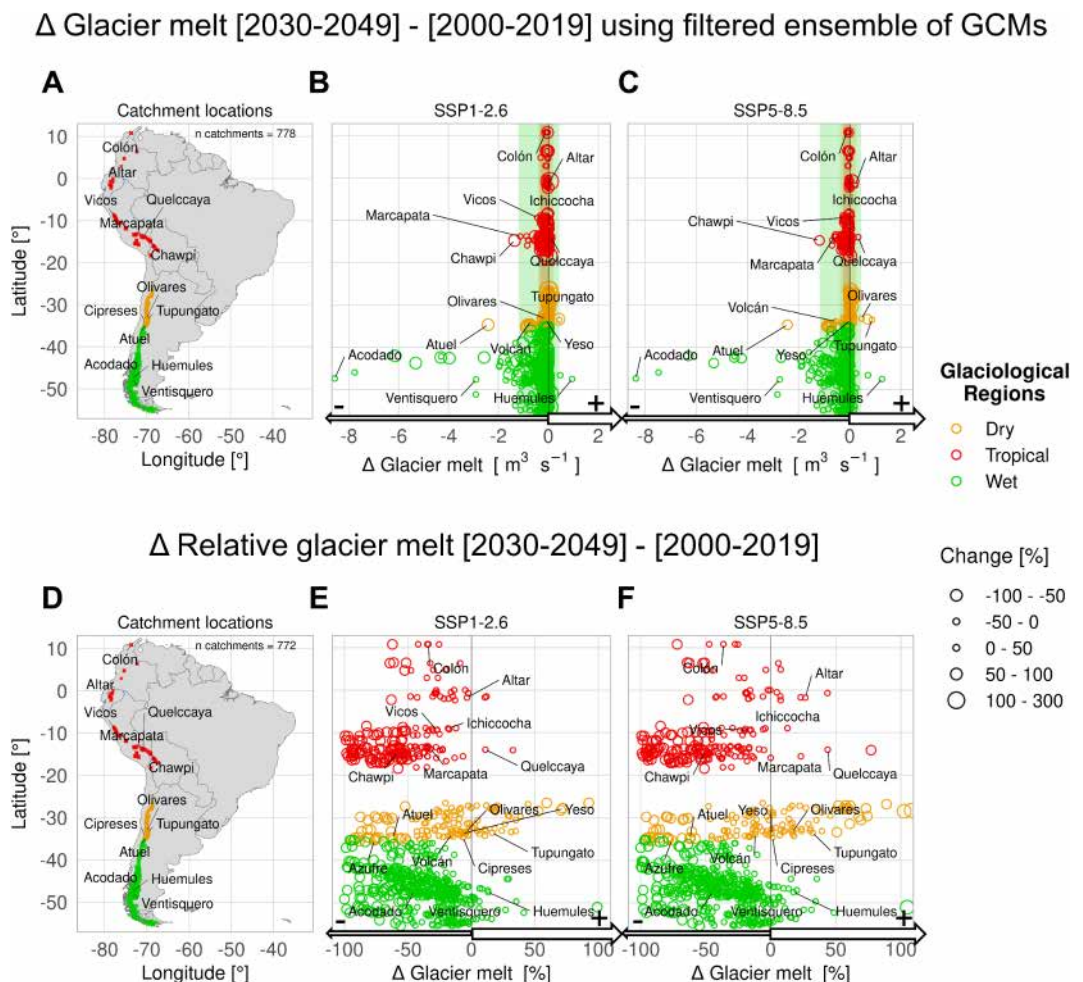


Fig. 2. Mean annual changes in glacier runoff between the periods 2000–2019 and 2030–2049 at the catchment scale using the filtered ensemble of GCMs. For the period 2000–2019 the cTC data are used in the simulations, whereas for the period 2030–2049 an ensemble of evaluated GCMs data is used. A) and D) show the location of all catchments and the other ones considered in relative values of changes, respectively. Glacier runoff differences are presented across the Andes (778 catchments) in absolute values of changes ($\text{m}^3 \text{ s}^{-1}$) for the SSP1-2.6 (B) and SSP5-8.5 scenarios (C). E) and F) represent glacier runoff changes in relative values between -100 and 100% . The vertical overlap of green, orange and red stripes in B and C display the standard deviation of glacier runoff changes by the Tropical, Dry, and Wet Andes. A similar figure using the complete ensemble can be found in Figure S3 of Supplementary Information.

these catchments exhibiting contrasting behavior. Regarding the spatial distribution of catchments, increases in glacier runoff are predominant in Argentine catchments, such as the Tupungato catchment. Conversely, the negative changes, which constitute the majority of the volume changes, are distributed evenly between Chile and Argentina. Noteworthy catchments in this category include the Azufre catchment and Atuel catchment.

Table 1 displays simulations of extreme glacier runoff changes in catchments using the SSP5-8.5 scenario, categorized by glaciological regions. These results provide insights into significant variations in glacier runoff. Across all regions, the Acodado catchment in the Wet Andes experiences the most substantial reduction in glacier runoff, with a decrease in $-8.4 \text{ m}^3 \text{ s}^{-1}$. Meanwhile, the Atuel catchment exhibits the largest reduction in percentage in the Dry Andes, with a reduction of -62% ($-2.4 \text{ m}^3 \text{ s}^{-1}$). These changes represent a considerable decline regarding their historical annual glacier runoff between 2000 and 2019.

Conversely, the Huemules, Tupungato, and Olivares catchments show the most substantial increases in glacier runoff. It is noteworthy that the eastern side of the Andes (Argentina) shows the most pronounced reductions and increases in glacier runoff, indicating potential impacts on water resources and hydrological systems in the Dry Andes. Comparatively, the Tropical Andes experience smaller extreme changes in glacier runoff compared to the other two glaciological regions, which can be attributed to relatively lower mean glacier runoff during the historical period. Notably, catchments such as Chawpi Urqu and Quelccaya display mean glacier runoff below $2.3 \pm 1.3 \text{ m}^3 \text{ s}^{-1}$ for the 2000–2019 period.

Glacier peak water throughout the 21st century

The peak water was explored in the period 2000–2099. The expected peak water (PW) estimation for 778 Andean catchments considering the filtered ensemble of GCMs within the SSP1-2.6 and SSP5-8.5 scenarios indicates that the maximum contribution of glacier runoff to river discharge will likely occur before the first half of the 21st century. Figure 3 illustrates the distribution of PW years (percentiles 25 and 75 in scenario SSP5-8.5), with a concentration between 2010 and 2028 across the Andes. The closest PW years to the present occur first in the Wet Andes (2010–2024, $n=465$ catchments), followed by the Tropical Andes (2014–2030, $n=183$ catchments), and finally in the Dry Andes (2021–2046, $n=130$ catchments). For the future period (2026–2099), PW years occur most frequently between 2026 and 2049. Tropical Andes will likely experience PW years in most catchments sooner (2026–2040, 50 to 86 catchments) than the Wet Andes (2030–2038, 40 to 30 catchments), and finally the Dry Andes (2030–2048, 82 to 110 catchments). Interestingly, in the Dry Andes, most catchments will likely show PW years later in the future (2026–2099). More details regarding the distribution of PW years by glaciological regions in SSP1-2.6 scenario of climate change can be found in Figure S6.

Specific locations in Fig. 3 and catchments in Table 2 provide a detailed view of the changes in PW year and the associated amounts of glacier runoff. These details allow for an examination of glacier runoff at the catchment scale within the SSP5-8.5 scenario.

In the Tropical Andes, catchments in Colombian Sierra Nevada de Santa Marta (e.g., Pico Colón) display PW years spanning from 2020 to 2028, with a maximum glacier runoff of $0.3 \text{ m}^3 \text{ s}^{-1}$. In Ecuador, PW years are projected to occur later in the second half of the 21st century, specifically from 2022 to 2084. Notably, the Altar catchment in Ecuador stands out, with a PW year estimated at 2052 ± 10 and a glacier runoff of $1.0 \text{ m}^3 \text{ s}^{-1}$. In Perú, cordilleras with significant glacierized areas would experience their PW year before the first half of the 21st century. The Cordillera Blanca shows PW years ranging from 2018 to 2064, while the Cordillera Vilcanota exhibits PW years from 2024 to 2050. The Marcapata catchment, located in the Cordillera Vilcanota, holds the largest estimated glacier runoff volume in the Tropical Andes at $3.0 \text{ m}^3 \text{ s}^{-1}$, with a PW year projected in 2030 ± 10 . The Dry Andes shows a range of PW years from 2010 to 2062. The largest glacier runoff is simulated in the Cipreses catchment ($9.3 \text{ m}^3 \text{ s}^{-1}$), followed by the Volcán catchment ($4.0 \text{ m}^3 \text{ s}^{-1}$), and the Olivares catchment ($3.6 \text{ m}^3 \text{ s}^{-1}$). For PW years simulated after 2049, larger glacier runoff volumes are observed in the Tupungato catchment ($4.0 \text{ m}^3 \text{ s}^{-1}$) and the Yeso catchment ($1.2 \text{ m}^3 \text{ s}^{-1}$). In contrast to the Tropical and Dry Andes, the

Catchment name	Mean annual Glacier runoff in the reference 2000–2019 [$\text{m}^3 \text{ s}^{-1}$]	Change of glacier runoff between 2030–2049 and 2000–2019 [$\text{m}^3 \text{ s}^{-1}$]	Change of glacier runoff between 2030–2049 and 2000–2019 [%]	Glaciological region	Country	Catchment id	Catchment area [km^2] Glacierized area (%)	Latitude
Negative changes								
Acodado	18.8 ± 2.1	-8.4	-45	Wet Andes	Chile	6,090,024,320	639 (26)	47°S
Atuel	4.0 ± 0.6	-2.4	-62	Dry Andes	Argentina	6,090,900,470	348 (14)	35°S
Chawpi Urqu	2.3 ± 1.3	-1.2	-45	Tropical Andes	Perú-Bolivia	6,090,601,720	198 (21)	15°S
Positive changes								
Huemules	7.2 ± 2	1.3	18	Wet Andes	Chile	6,090,965,210	207 (43)	48°S
Tupungato	2.7 ± 1.0	0.9	32	Dry Andes	Argentina	6,090,891,240	289 (28)	34°S
Olivares	2.7 ± 1.1	0.5	16	Dry Andes	Chile	6,090,889,690	534 (14)	33°S
Quelccaya	0.8 ± 0.4	0.3	45	Tropical Andes	Perú	6,090,582,670	182 (9)	14°S

Table 1. Maximum reductions and increases in glacier runoff identified by catchment using scenario SSP5-8.5 of filtered ensemble between the periods 2000–2019 and 2030–2049 across the Andes.

Andean peak water 2000-2099 SSP5-8.5

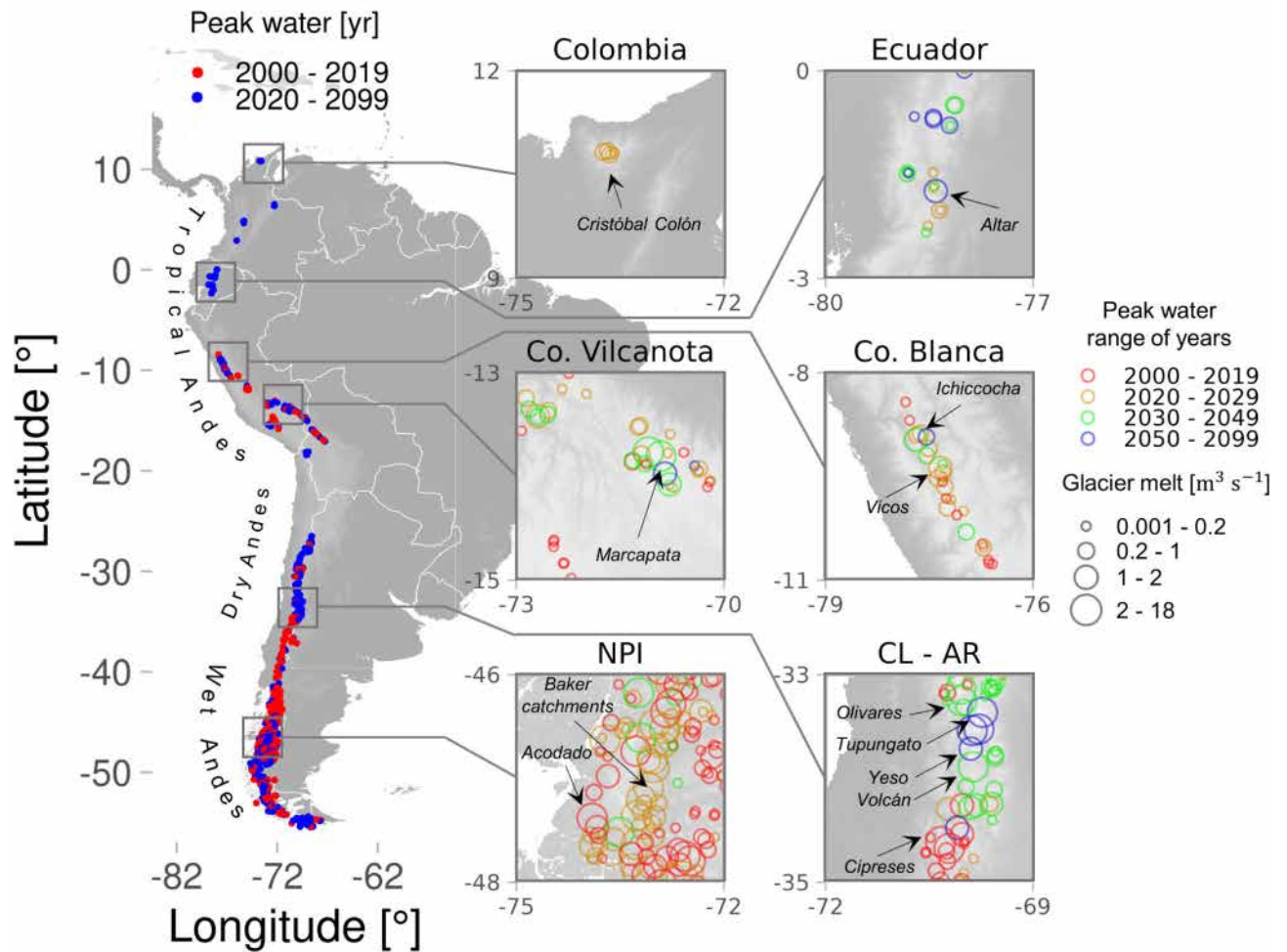


Fig. 3. Peak water year and related mean annual glacier runoff across the Andes for the SSP5-8.5 scenario throughout the 21st century. In the South American map, the peak water per catchment is exhibited for the “current” period (2000–2025 in red) and for the future (2026–2099, blue), using simulations forced by the filtered ensemble of GCMs. Detailed maps can be seen in six locations from the Sierra Nevada de Santa Marta in Colombia to the Northern Patagonian Icefield in Chile. The CL-AR location shows central Chile and Argentina. The figure using the SSP1-2.6 scenario can be found in Figure S6 of Supplementary Information.

Wet Andes region exhibits significant amounts of glacier runoff. Catchments in the Wet Andes, particularly in the latitudinal range of 46–48°S, considering the land-terminating glaciers of Northern Patagonian Icefield and surrounding glaciers, show a PW year range before the mid of the 21st century, from 2010 to 2048. The Acodado catchment situated on the west side of the Andes stands out with the highest maximum glacier runoff of $17.8 \text{ m}^3 \text{s}^{-1}$ and a PW year of 2010 ± 10 . On the eastern side of the Northern Patagonian Icefield, catchments related to the Baker basin are estimated to experience PW years before 2030. Among these catchments, the Soler catchment (in the NPI) exhibits a larger PW volume of $8.5 \text{ m}^3 \text{s}^{-1}$ compared to those found east of the NPI, like the Maitén catchment, with a runoff of $0.9 \text{ m}^3 \text{s}^{-1}$. From this analysis, we conclude that the calculation of the PW for each catchment is crucial in characterizing the local differences and spatial variability observed in the Andes. These diverse behaviors are attributed to the distinct morphometric characteristics of land-terminating glaciers and local climates in each catchment.

The annual and monthly temporal series of glacier runoff for each glacier and catchment are available in the Supplementary data. For more in-depth information and specific examples, refer to Figures S7, S8 and S9, in the Supplementary information. These figures present the detailed temporal variations in glacier runoff for the respective glaciers and catchments.

Discussion

Assessment of climate evolution from GCMs

Presently, a comprehensive evaluation of GCMs outputs in glacierized catchments across the Andes is notably lacking, encompassing both CMIP6 and earlier datasets. Consequently, the prevailing reference source

Catchment name	PW year	PW glacier runoff [m ³ s ⁻¹]	Location	Country	Catchment id	Catchment area [km ²] Glacierized area (%)	Latitude
Pico Cristóbal Colón	2024 ± 10	0.3 ± 0.02	Colombia	Colombia	6,090,000,970	696 (1)	11°N
Altar	2052 ± 10	1.0 ± 0.04	Ecuador	Ecuador	6,090,249,220	668 (3)	2°S
Vicos	2020 ± 10	1.5 ± 0.05	Co. Blanca	Perú	6,090,461,650	279 (19)	9°S
Ichiccocha	2030 ± 10	1.2 ± 0.06	Co. Blanca	Perú	6,090,449,220	246 (13)	9°S
Marcapata	2030 ± 10	3.0 ± 0.09	Co. Vilcanota	Perú	6,090,571,030	730 (14)	14°S
Olivares	2040 ± 10	3.6 ± 0.18	CL-AR	Chile	6,090,889,690	534 (14)	33°S
Tupungato	2058 ± 10	4.0 ± 0.09	CL-AR	Argentina	6,090,891,240	289 (28)	34°S
Yeso	2054 ± 10	1.2 ± 0.02	CL-AR	Chile	6,090,892,710	627 (6)	34°S
Volcán	2040 ± 10	4.0 ± 0.06	CL-AR	Chile	6,090,892,940	524 (14)	34°S
Cipreses	2010 ± 10	9.3 ± 0.23	CL-AR	Chile	6,090,897,370	350 (33)	35°S
Soler	2026 ± 10	8.5 ± 0.24	NPI	Chile	6,090,963,530	749 (16)	47°S
Maitén	2010 ± 10	0.9 ± 0.05	East of NPI	Chile	6,090,962,900	386 (7)	47°S
Acodado	2010 ± 10	17.8 ± 0.39	NPI	Chile	6,090,024,320	639 (26)	47°S

Table 2. Catchments highlighted by glacier runoff during the identified peak water year between 2000–2099 across the Andes.

has been the IPCC AR6 report²⁸, which examined climate variations in the Andes utilizing over 30 CMIP6 GCMs. Nevertheless, a key distinction between our simulations, focused on glaciers, and the IPCC report is the treatment of regional extension, wherein the latter considers a broader land area beyond the glacierized surfaces and situated at lower elevations. IPCC²⁸ indicates an overall temperature increase for all scenarios, with the northern half of the continent experiencing more substantial warming, gradually decreasing southward. Additionally, precipitation is anticipated to decrease over the Dry and Wet Andes while increasing over the Tropical Andes during the period 2041–2060, taking 1995–2014 as a reference period (under the SSP5-8.5 scenario). This pattern is consistent with the findings of Almazroui et al.²⁹ who evaluated an ensemble of CMIP6 models across South America. Moreover, the GCMs ensemble tends to underestimate precipitation during the rainiest months while overestimating it during the drier months in the Dry and Wet Andes²⁹. In agreement with the IPCC under the SSP5-8.5 scenario, our results confirm a maximum temperature increase in the Tropical Andes (1.9 °C), followed by the Dry (1.5 °C), and Wet Andes (1.1 °C, southward of NPI) during the period 2030–2049. For precipitation, the IPCC reports a reduction in the Dry Andes (-8%) and Wet Andes (-0.1%), alongside an increase in the Tropical Andes (4.5%)²⁸. However, our findings diverge, showing a negative trend in the Tropical and Wet Andes. Notably, precipitation only exhibits an increase in the SSP1-2.6 scenario for the Tropical Andes.

Regarding the Tropical Andes and the northern area of the Dry Andes, Olmo et al.³⁰ conducted a study focusing on the representation of precipitation variability in the July–October season (1979–2014). By using the CESM2 and MPI-ESM1-2-HR models from CMIP6, they indicated that these models effectively capture the underlying physical mechanisms governing precipitation patterns. Our analysis revealed that these same models exhibit a high monthly correlation but a poor seasonal correlation for the OND season. However, in the Dry Andes region (18–37°S), these models exhibit a robust seasonal correlation, which holds significant importance for glacier mass balance simulations.

Regarding future projections, we observed a median reduction in precipitation during the JAS and OND seasons (as projected by MPI, CESM2, and NorESM2-MM) under the SSP1-2.6 and SSP5-8.5 scenarios. These results are in line with estimations made by Agudelo et al.³¹ which indicate an increase in the occurrence of dry days (19.4%) during the austral winter (JAS) and a higher frequency of dry circulation patterns during the July–October period. Notably, the CESM2 model demonstrated the most favorable outcomes concerning precipitation variability over the southwestern region during the historical period (1901–2014) as indicated by Rivera and Arnould³².

Given the foregoing, the use of GCMs as input data in future glacier runoff simulations should consider the following aspects. First, the importance of seasonal evaluation. Indeed, it is crucial to assess GCM performance during critical periods of glacier melt because neglecting seasonal evaluations in favor of monthly or annual assessments may overlook deficiencies in seasonal performance. Second, the GCM performance over glacierized areas must be evaluated. Indeed, using GCMs evaluated for other types of land covers could present seasonal variations that are not representative of glacierized regions but of lower elevations.

Uncertainties associated with glacier evolution

Three important aspects in the glacier dynamics considered in the simulations using OGGM need to be discussed to account for the likelihood of the presented results:

- The approach based on the Shallow Ice Approximation (SIA), implemented in OGGM, lacks longitudinal/transverse stress gradients and other complex mechanisms of glacier dynamics³³. Because of that simulated

glaciers across the Andes could miss ice dynamics responses, and for example accelerating their melting rates throughout the century. This issue could be addressed using higher-order ice flow models³⁴, which are better suited for accurately representing ice flow. However, these models are computationally challenging to implement across the vast, glacierized expanse of the Andes³⁵.

- ii) The ice thickness calibration in this study relies on data from Farinotti et al.²⁵, which employs an ensemble of up to five models to estimate the ice thickness distribution. Unfortunately, this approach leads to an overestimation of approximately 20% (median) of the measured ice thickness. Moreover, our calibration parameter values for ice thickness align with values from Cuffey and Paterson³⁶ and Millan et al.³⁷. The simulations predict lower Glen A parameter values for glaciers with lower internal temperatures, such as those found in the glaciological zone DA1 ($2.4 \times 10^{-25} \text{ s}^{-1} \text{ Pa}^{-3}$), which represents the coldest zone in the Andes. Additionally, Millan et al.³⁷ estimated Glen A parameters in the Andes ranging between 6×10^{-25} and $2 \times 10^{-24} \text{ s}^{-1} \text{ Pa}^{-3}$, while the calibrated values used in this study range from 2×10^{-25} and $2 \times 10^{-23} \text{ s}^{-1} \text{ Pa}^{-3}$.
- iii) Due to the limitations mentioned in (i) and (ii), our simulations of future glacier runoff changes carry uncertainties arising from the ice thickness simulation and its calibration. Moreover, the climate performance in the historical period and the various climate models and scenarios considered contribute to the overall uncertainty. Estimating melt factor values is also critical. However, we minimized biases in the glacier mass balance simulation by calibrating the melt factors, which were derived using corrected climate datasets from Caro et al.⁴, along with the geodetic mass balance data from Hugonnet et al.¹¹.

The three main sources of uncertainty in future simulations of glacier runoff are: (i) the SIA, (ii) the calibration of glacier volume, and (iii) the use of GCMs and parameter values for mass balance estimation. Despite simulation biases, simulations at the Andes scale capture variations in future glacial runoff between catchments and Andean regions which sound coherent with current spatio-temporal differences. This capability arises from a consistent modeling approach, calibrated and validated across the Andes using historical data, and gives confidence for a well-calibrated global glaciological model, such as OGGM, to be used at regional scale. Also, it incorporates the highest-scored climate projections specific to each region for future simulations.

PW estimation across the Andes

Our 21st century PW estimates partially align with Huss and Hock⁸ findings. They identified PW in 12 Andean basins with a glacierized surface area of 9,544 km² (considering land-terminating glaciers), representing different proportions in the Tropical Andes (23%), Dry Andes (20%) and Wet Andes (57%). Their results revealed a PW already past in the inner tropics (2 catchments) and projected a PW occurrence between 2011 and 2046 in the outer tropics (4 catchments). In the Dry Andes, the estimated PW was around 2010 ± 24 (2 catchments in western side), while the Wet Andes showed a broader range from 2003 ± 11 to 2096 ± 24 (4 catchments). Interestingly, they found evidence of past PW in the northern area of the Wet Andes. In contrast, our estimations considered a larger glacierized surface area (11,282 km², excluding calving glaciers concentrated in the Patagonian icefields). More details can be seen in section Data and Methods. Our results suggest that the PW will occur before the first half of the 21st century in the majority of the catchments across the Andes. The PW has already occurred in most of the Tropical Andes catchments and will occur before 2049 in most of the Dry Andes catchments. In the Wet Andes, the majority of catchments experienced PW before the present day. These peak water occurrences can be observed from both scenarios of climate change across the Andes. Generally, an earlier PW occurrence is associated with less warm scenarios, which aligns with observations in the Himalayan mountains and specific Andean catchments^{8,38}.

Understanding the timing of peak water occurrence is essential for effective water supply management in glacierized catchments, especially those with prolonged dry seasons. As highlighted by Caro et al.⁴, the La Paz (17°S) and Maipo (33°S) catchments experience distinct seasonal patterns, with extreme wet/cold and dry/warm periods. In these regions, glaciers play a crucial role in maintaining river flow during the dry season, contributing 15% and 34% of streamflow, respectively. Furthermore, assessing the impact of decreased glacier runoff requires considering factors such as catchment scale, glacierized area, and snow cover. This goal must integrate glacier runoff estimations with hydrological models³⁹.

Conclusion

We analyzed eight GCMs from CMIP6 to identify those best at reproducing historical climate (1990–2019) and projected future conditions (2020–2049) across the Andes. These models were then used to estimate changes in glacier runoff (2023–2049) and peak water throughout the 21st century (10°N–55°S) using the calibrated and validated Open Global Glacier Model (OGGM). For the first time, we conducted a comprehensive simulation of future glacier dynamics and runoff in 778 Andean catchments. We conclude the following:

- The filtered ensemble, which includes only the highest-scoring GCMs, offers a more accurate comparison at regional and catchment scales compared to the full ensemble of all GCMs. Although both ensembles simulate similar changes in glacier runoff at the Andean scale between the periods 2000–2019 and 2030–2049 under both climate change scenarios (SSP1-2.6 and SSP5-8.5), differences emerge at a more detailed level. Some catchments in the Dry Andes show discrepancies of up to 14% in the glacier runoff. These differences between both ensembles become more pronounced when comparing the mean glacier runoff in the period 2030–2049, with variations reaching as high as 7% in the Dry Andes and up to 50% in certain catchments.
- The cumulative glacier runoff loss in the Dry Andes is projected to reach 38%, while in the Tropical Andes, it is expected to be 43% between the periods 2000–2019 and 2030–2049. Notably, exceptional catchments in the Dry Andes, such as Tupungato (Argentina) and Olivares (Chile), exhibit an increase in glacier runoff of at

least 16%. Additionally, the variability in glacier runoff change across catchments is highlighted, ranging from a notable reduction in the Atuel (-62%) to an increase in the Tupungato catchment (+32%).

- Projections indicate that the peak water from glacier runoff will occur in most Andean catchments before the mid-21st century (between 2010 and 2028). Nevertheless, the distribution of PW years exhibits significant variations in Andean regions and catchments. The Wet Andes is expected to experience the earliest PW years (2010 to 2024), followed by the Tropical Andes (2014 to 2030), and the Dry Andes later (2021–2046).
- Special attention should be given to catchments that show the highest amounts of glacier runoff related to peak water, as estimated in the past (Cipreses catchment with $9.3 \text{ m}^3 \text{ s}^{-1}$ in 2010 ± 10) and in the short term (Volcán catchment with $4.0 \text{ m}^3 \text{ s}^{-1}$, and Olivares catchment with $3.6 \text{ m}^3 \text{ s}^{-1}$ in 2040 ± 10). In the Dry Andes, where these catchments are either decreasing or increasing their glacier runoff contribution to the river, this could be critical for water supplies to social-ecological systems, particularly during the dry season, especially in years of drought.

Finally, this study offers a comprehensive analysis of glacier runoff variations for the first half of the 21st century. It underscores the urgent need to account for regional and catchment specific differences when designing water resource adaptation strategies, particularly in the context of anticipated changes in glacier contributions. To enhance these strategies, future work should focus on more detailed assessments of glacier contributions in key catchments, incorporating improvements in simulation accuracy through the integration of hydro-climate measurements.

Data and methods

Analysis of the GCMs in the historical and future periods

In this study, we analyze temperature and precipitation data from two scenarios and selected GCMs simulations sourced from CMIP6 (see Table S5). Our GCMs selection takes into account the Almazroui et al.²⁹ assessment for GCMs in South America and the global evaluation of warmer models from Hausfather et al.²¹ and Tokarska et al.²³. To establish a basis for comparison, we bias corrected the GCMs simulations using the method implemented in the OGGM model, and then we compared the bias corrected GCMs with the corrected TerraClimate variables⁴⁰. TerraClimate have been corrected for temperature and precipitation (cTC, temperature, and precipitation) at the scale of the Andes on the basis of in situ data from 34 meteorological stations⁴ during the historical period of 1990–2019 across the Andes on a glacierized area of 27,668 km² (considering glaciers with a surface area > 1 km²). Meanwhile, we also perform comparisons between GCMs during both the historical and future periods (2020–2049). Our analysis comprises three steps: step 1: statistical downscaling of GCMs temperature and precipitation data for the historical period; step 2: calculation of annual, seasonal and monthly metrics to compare the GCMs data with the corrected TerraClimate data for the historical period; and step 3: Identification of changes in climate variables between the historical and future periods. Such simulations were deemed impossible to conduct in this context. Going into detail, these three steps consist in:

- Step (1) The mean monthly and annual values of temperature and precipitation from the GCMs were adjusted to the mean elevation of each glacier. This adjustment was performed using a statistical downscaling approach for two future scenarios (SSP1-2.6 and SSP5-8.5), based on the historical climate data from the cTC (1990–2019).
- Step (2) Correlation pattern analyses were based on monthly and seasonal (OND, JFM, AMJ, JAS) correlations between the eight GCMs and the cTC data in the period 1990–2019. We chose seasons as OND and JFM, because in these months the larger surface mass loss occurs in the Outer Tropics (transition season⁴¹) and in the Dry Andes zones (austral summer). We used the Pearson coefficient of correlation and the root mean square error (RMSE)⁴² as metrics to score the GCMs performance during the historical period.
- Step (3) We identified climate likely ranges through the GCMs ensemble considering the mean differences between the historical and future periods for temperature and precipitation at annual and seasonal (OND, JFM, AMJ, JAS) time-steps in each glacier. The climate change likely ranges are estimated by the percentiles 10 and 90 of these differences using all GCMs and glaciers (modified from DRIAS project⁴³). In addition, we estimate the median of these differences. A similar method is used by the DRIAS project of the *Ministère de la Transition Écologique* of the French government (see Table S2, DRIAS project⁴³, and Sørland et al.⁴⁴). The annual analysis between the historical and future periods (2020–2049 and 2070–2099) is considered to test our results with previous reports of climate change (e.g., IPCC²⁸, Olmo et al.³⁰, and Agudelo et al.³¹). The estimation of the climate change likely ranges allows us to identify four types of models: the hot/dry; the cold/dry; the hot/wet and the cold/wet models.

After these steps, we defined a complete ensemble considering eight GCMs, and a second GCM ensemble that comprise highly score GCMs, called filtered ensemble.

The GCMs output data were gathered for each glacier. However, the analysis was performed at the glaciological region scale, where climate characteristics vary substantially⁴⁵. We did not include glaciers experiencing mass loss due to calving in our simulations conducted in the Patagonian region⁴⁶.

Short description of the Open Global Glacier Model (OGGM)

OGGM is a modular and open-source workflow that simulates glacier mass balance and ice dynamics using calibrated parameter values for each glacier²⁴. The required input data are: air temperature and precipitation time series, glacier outlines and surface topography. From these inputs, annual (e.g., surface mass balance, glacier volume and area) and monthly (glacier melt [snow + ice] and rainfall on glaciers) outputs can be simulated.

Using a glacier outline and topography, OGGM estimates flow lines using a geometrical algorithm (adapted from Kienholz et al.⁴⁷). Assuming a bed shape, it estimates the ice thickness based on mass conservation and shallow ice approximation²⁴. After these numerical steps, area and volume per glacier can be simulated. Mass balance is implemented using a precipitation phase partitioning and a temperature-index approach^{6,48–50}. The monthly mass balance mb_i at an elevation z is computed as follows:

$$mb_i(z) = TC_{pi}^{snow}(z) * P_f - M_f * \max(cTC_{ti}(z) - T_{melt}, 0), \quad (1)$$

where TC_{pi}^{snow} is the TerraClimate solid precipitation before being scaled by the precipitation correction factor (P_f), M_f is the glacier's temperature sensitivity parameter, cTC_{ti} is the monthly corrected TerraClimate temperature, and T_{melt} is the monthly air temperature above which ice melt is assumed to occur (from 0 °C to 2.1 °C). TC_{pi}^{snow} is computed as a fraction of the total precipitation (cTC_p) where 100% is getting if $cTC_{ti} \leq T_i^{snow}$ (between 0 and 2.1 °C) and 0% if $cTC_{ti} \geq T_i^{rain}$ (between 2 and 4.1 °C); and linearly interpolated in between. Here, the M_f was calibrated for each glacier individually using glacier volume change datasets previously described¹¹.

Model setup in the period 2000–2050

The OGGM model was previously calibrated and evaluated during the period 2000–2019 across the Andes (10°N–55°S) in a former study by Caro et al.⁴. In this former study, we evaluated and corrected temperature and precipitation input data, evaluated the simulated glacier mass balances outputs using in situ mass balance measurements, and also the model performance at the level of three Andean catchments.

The model was run for each glacier and then results were analyzed for each glaciological zone identified by Caro et al.⁴⁵ across the Andes. During the historical (2000–2019) and future (2020–2050) periods the input data are: glacier outlines from RGI v6.0⁵¹ and surface topography from NASADEM⁵². The corrected monthly TerraClimate precipitation (cTC_p) and temperature (cTC_t) were used in the historical period. Following the methodology of Caro et al.⁴, glaciers from the RGI v6.0 dataset were filtered to exclude calving glaciers. This exclusion was necessary as the OGGM model cannot simulate glaciers with frontal ice loss due to calving, which are predominantly found in the Wet Andes. Consequently, 36% (11,000 km²) of the total glacierized area in the Andes was considered. In the Dry Andes (18–37°S) and Tropical Andes (11°N–18°S), over 80% of the glacierized area was included in the analysis. For the Wet Andes (37–55°S), 29% of the glacierized surface area was considered, representing 26% (8000 km²) of the total glacierized area in the Andes.

For the future period, monthly precipitation and temperature were selected from eight GCMs. These variables were used as input for the future simulations. The calibration procedure was applied for each individual glacier to adjust the simulated mass balance of the 2000–2019 period to the geodetic mass balance product from Hugonnet et al.¹¹. The simulated glacier volume was calibrated using Farinotti et al.²⁵ product at a glaciological zone scale fitting the A parameter of the Glen flow law. In addition, glacier outlines of all glaciers were associated with the year 2000. The main corrected and calibrated parameters to run OGGM across the Andes are summarized in Table S6.

Glacier runoff changes were estimated by adding the annual melt from each glacier by catchment, for this we considered the centroid of each glacier contour. From this annual glacier runoff time series, the difference of the mean annual glacier runoff between the periods 2000–2019 and 2030–2049 was estimated for 778 glacierized catchments. Meanwhile, PW refers to the annual glacier runoff that will initially increase and after declining in response to glacier retreat due to changes in climate conditions⁸ which can be for example a long-term response of catchments to sustained warming⁵³. We calculate the PW inspired by Huss and Hock⁸ through the following procedure by glacier and after by catchment: (i) A maximum of eight time series of the simulated glacier runoff from each glacier are compiled. Each time series comes from the different OGGM runs using different GCMs (the number of GCMs varies between the filtered and complete ensembles in each glaciological region); (ii) Then, the time series were averaged, getting one time series of glacier runoff per glacier; (iii) these were summed annually by catchment, allowing us to obtain the annual glacier runoff in each catchment between 2000 and 2099; (iv) The glacier runoff was smoothed using a moving average comprising 11 years; (v) On these smoothed time-series we selected the period of 20 years related to maximum glacier runoff; (vi) Finally, the PW year corresponds to the median of these 20 years with a fixed uncertainty range of +/- 10 years. We considered the 20 years of uncertainty from the period where the model where calibrated between 2000 and 2019⁴.

Data availability

All data analyzed in this article are available by glacier and catchment at <https://zenodo.org/records/12714725>. Other data such as the catchment outlines and their identifier (id) are available at <https://doi.org/10.5281/zenodo.7890462>, related to the article “Hydrological response of Andean catchments to recent glacier mass loss” <https://doi.org/10.5194/tc-18-2487-2024>.

Received: 10 July 2024; Accepted: 23 January 2025

Published online: 31 March 2025

References

1. Buytaert, W. et al. Glacial melt content of water use in the tropical Andes. *Environ. Res. Lett.* **12** (11). <https://doi.org/10.1088/1748-9326/aa926c> (2017).

2. Ayala, Á. et al. Glacier runoff variations since 1955 in the Maipo River basin, in the semiarid Andes of central Chile. *Cryosphere* **14**, 2005–2027. <https://doi.org/10.5194/tc-14-2005-2020> (2020).
3. Poveda, G. et al. High Impact Weather events in the Andes. *Front. Earth Sci.* **8**, 162. <https://doi.org/10.3389/feart.2020.00162> (2020).
4. Caro, A. et al. Hydrological Response of Andean Catchments to Recent Glacier Mass Loss. *The Cryosphere*; (2024). <https://doi.org/10.5194/tc-18-2487-2024>
5. Drenkhan, F. et al. Looking beyond glaciers to understand mountain water security. *Nat. Sustain.* **6** (February), 130–138. <https://doi.org/10.1038/s41893-022-00996-4> (2023).
6. Marzeion, B., Jarosch, A. H. & Hofer, M. Past and future sea-level change from the surface mass balance of glaciers. *Cryosphere* **6**, 1295–1322. <https://doi.org/10.5194/tc-6-1295-2012> (2012).
7. Radic, V. & Hock, R. Glaciers in the Earth's hydrological cycle. Assessments of glacier mass and runoff changes on global and regional scales. *Surv. Geophys.* **35**, 813–837. <https://doi.org/10.1007/s10712-013-9262-y> (2014).
8. Huss, M. & Hock, R. Global-scale hydrological response to future glacier mass loss. *Nat. Clim. Change* **8**, 135–140. <https://doi.org/10.1038/s41558-017-0049-x> (2018).
9. Rounce, D. et al. Global glacier change in the 21st century: every increase in temperature matters. *Science* **379**, 78–83. <https://doi.org/10.1126/science.abo1324> (2023).
10. Zekollari, H. et al. Twenty-first century global glacier evolution under CMIP6 scenarios and the role of glacier-specific observations. *Cryosphere* **18**, 5045–5066. <https://doi.org/10.5194/tc-18-5045-2024> (2024).
11. Hugonnet, R. et al. Accelerated global glacier mass loss in the early twenty-first century. *Nature* **592**, 726–731. <https://doi.org/10.1038/s41586-021-03436-z> (2021).
12. Aschwanden, A., Aðalgeirsdóttir, G. & Khroulev, C. Hindcasting to measure ice sheet model sensitivity to initial states. *The Cryosphere* **7**; (2013). <https://doi.org/10.5194/tc-7-1083-2013>
13. Huss, M. & Hock, R. A new model for global glacier change and sea-level rise. *Front. Earth Sci.* **3**, 54. <https://doi.org/10.3389/feart.2015.00054> (2015).
14. Vuille, M. et al. Rapid decline of snow and ice in the tropical Andes—Impacts, uncertainties and challenges ahead. *Earth Sci. Rev.* **176**, 195–213. <https://doi.org/10.1016/j.earscirev.2017.09.019> (2018).
15. Réveillet, M., Rabatel, A., Gillet-Chaulet, F. & Soruco, A. Simulations of changes to Glacier Zongo, Bolivia (16S), over the 21st century using a 3-D full-Stokes model and CMIP5 climate projections. *Ann. Glaciol.* **56**, 89–97. <https://doi.org/10.3189/2015aog70a113> (2015).
16. Frans, C. et al. Predicting glacio-hydrologic change in the headwaters of the Zongo River, Cordillera Real, Bolivia. *Water Resour. Res.* **51**, 9029–9052. <https://doi.org/10.1002/2014WR016728> (2015).
17. Scheiter, M., Schaefer, M., Flández, E., Bozkurt, D. & Greve, R. The 21st-century fate of the Mocho-Choshuenco ice cap in southern Chile. *Cryosphere* **15**, 3637–3654. <https://doi.org/10.5194/tc-15-3637-2021> (2021).
18. Schaefer, M., MacHuth, H., Falvey, M. & Casassa, G. Modeling past and future surface mass balance of the Northern Patagonia icefield. *J. Geophys. Res. Earth Surf.* **118**, 571–588. <https://doi.org/10.1002/jgrf.20038> (2013).
19. Bravo, C. et al. Projected increases in surface melt and ice loss for the Northern and Southern Patagonian Icefields. *Sci. Rep.* **11**, 16847. <https://doi.org/10.1038/s41598-021-95725-w> (2021).
20. Marzeion, B. et al. Partitioning the uncertainty of Ensemble projections of Global Glacier Mass Change. *Earth's Future* **8**, 1010292019EF001470 (2020).
21. Hausfather, Z., Marvel, K., Schmidt, G. A., Nielsen-Gammon, J. W. & Zelinka, M. Climate simulations: recognize the 'hot model' problem. *Nature* **605**, 26–29. <https://doi.org/10.1038/d41586-022-01192-2> (2022).
22. Eyring, V. et al. Overview of the coupled model Intercomparison Project Phase 6 (CMIP6) experimental design and organization. *Geosci. Model. Dev.* **9**, 1937–1958. <https://doi.org/10.5194/gmd-9-1937-2016> (2016).
23. Tokarska, K. B. et al. Past warming trend constrains future warming in CMIP6 models. *Sci. Adv.* **6**, eaaz9549. <https://doi.org/10.1126/sciadv.aaz9549> (2020).
24. Maussion, F. et al. The open global glacier model (OGGM) v1.1. Geoscientific model. *Develop* **12**, 909–931. <https://doi.org/10.5194/gmd-12-909-2019> (2019).
25. Farinotti, D. et al. A consensus estimate for the ice thickness distribution of all glaciers on Earth. *Nat. Geosci.* **12**, 168–173. <https://doi.org/10.1038/s41561-019-0300-3> (2019).
26. Aguayo, R. et al. Unravelling the sources of uncertainty in glacier runoff projections in the Patagonian Andes (40–56° S). *Cryosphere* **18**, 5383–5406. <https://doi.org/10.5194/tc-18-5383-2024> (2024).
27. Rabatel, A. et al. Current state of glaciers in the tropical Andes: a multi-century perspective on glacier evolution and climate change. *Cryosphere* **7** (1), 81–102. <https://doi.org/10.5194/tc-7-81-2013> (2013).
28. IPCC AR6. IPCC WGI Interactive Atlas. Regional information (Advanced). (2022). <https://interactive-atlas.ipcc.ch/>
29. Almazroui, M. et al. Assessment of CMIP6 performance and projected temperature and precipitation changes over South America. *Earth Syst. Environ.* **5**, 155–183. <https://doi.org/10.1007/s41748-021-00233-6> (2021).
30. Olmo, M. E. et al. Circulation patterns and associated rainfall over south tropical South America: GCMs evaluation during the dry-to-wet transition season. *J. Geophys. Res. Atmos.* **127** <https://doi.org/10.1029/2022JD036468> (2022).
31. Agudelo, A. et al. Future projections of low-level atmospheric circulation patterns over South Tropical South America: impacts on precipitation and Amazon dry season length. *J. Geophys. Research: Atmos.* <https://doi.org/10.1029/2023JD038658> (2023). .128, e2023JD038658.
32. Rivera, J. A. & Arnould, G. Evaluation of the ability of CMIP6 models to simulate precipitation over Southwestern South America: climatic features and long-term trends (1901–2014). *Atmos. Res.* **241**, 104953. <https://doi.org/10.1016/j.atmosres.2020.104953> (2020).
33. Le Meur, E., Gagliardini, O., Zwinger, T. & Ruokolainen, J. Glacier flow modelling: a comparison of the shallow ice approximation and the Full-Stokes solution. *C.R. Phys.* **5** (7), 709–722. <https://doi.org/10.1016/j.crhy.2004.10.001> (2004).
34. Oerlemans, J. Minimal Glacier Models (Utrecht Publishing and Archiving Services) (2008).
35. Juvet, G. et al. Deep learning speeds up ice flow modelling by several orders of magnitude. *J. Glaciol.* **68** (270), 651–664. <https://doi.org/10.1017/jog.2021.120> (2022).
36. Cuffey, K. & Paterson, W. The Physics of Glaciers (Academic Press) 4th edn. (2010).
37. Millan, R. et al. Ice velocity and thickness of the world's glaciers. *Nat. Geosci.* **15**, 124–129. <https://doi.org/10.1038/s41561-021-00885-z> (2022).
38. Laha, S., Banerjee, A., Singh, A., Sharma, P. & Thamban, M. The control of climate sensitivity on variability and change of summer runoff from two glacierised himalayan catchments preprint. *Hydrol. Earth Syst. Sci. Dis.* <https://doi.org/10.5194/hess-2021-499> (2021).
39. Hanus, S. et al. Coupling a large-scale glacier and hydrological model (OGGM v1.5.3 and CWatM V1.08) – towards an improved representation of mountain water resources in global assessments. *Geosci. Model. Dev.* **17**, 5123–5144. <https://doi.org/10.5194/gmd-17-5123-2024> (2024).
40. Abatzoglou, J. T., Dobrowski, S. Z., Parks, S. A. & Hegewisch, K. C. TerraClimate, a High-Resolution Global Dataset of Monthly Climate and Climatic Water Balance from 1958–2015. *Sci. Data* **5**, 1–12. ; <https://doi.org/10.1038/sdata.2017.191> (2018).

41. Autin, P., Sicart, J. E., Rabatel, A., Soruco, A. & Hock, R. Climate controls on the interseasonal and interannual variability of the Surface Mass and Energy balances of a Tropical Glacier (Zongo Glacier, Bolivia, 16° S): New insights from the multi-year application of a distributed Energy Balance Model. *J. Geophys. Research: Atmos.* **127** (7). <https://doi.org/10.1029/2021JD035410> (2022).
42. McSweeney, C. F., Jones, R. G., Lee, R. W. & Rowell, D. Selecting CMIP5 GCMs for downscaling over multiple regions. *Clim. Dyn.* **44** (11–12), 3237–3260. <https://doi.org/10.1007/s00382-014-2418-8> (2015).
43. DRIAS. DRIAS les futurs du climat; (2023). <http://drias-climat.fr>
44. Sørland, S. L., Schär, C., Lüthi, D. & Kjellström, E. Bias patterns and climate change signals in GCM-RCM model chains. *Environ. Res. Lett.* **13**, 074017. <https://doi.org/10.1088/1748-9326/aacc77> (2018).
45. Caro, A., Condom, T. & Rabatel, A. Climatic and morphometric explanatory variables of Glacier Changes in the Andes (8–55°S): New insights from Machine Learning approaches. *Front. Earth Sci.* <https://doi.org/10.3389/feart.2021.713011> (2021).
46. Minowa, M., Schaefer, M., Sugiyama, S., Sakakibara, D. & Skvarca, P. Frontal ablation and mass loss of the Patagonian Icefields. *Earth Planet. Sc Lett.* **561**, 116811. <https://doi.org/10.1016/j.epsl.2021.116811> (2021).
47. Kienholz, C., Rich, J. L., Arendt, A. A. & Hock, R. A new method for deriving glacier centerlines applied to glaciers in Alaska and northwest Canada. *Cryosphere* **8**, 503–519. <https://doi.org/10.5194/tc-8-503-2014> (2014).
48. Braun, L. N. & Renner, C. B. Application of a conceptual runoff model in different physiographic regions of Switzerland. *Hydrol. Sci. J.* **37** (3), 217–231. <https://doi.org/10.1080/02626669209492583> (1992).
49. Hock, R. Temperature index melt modelling in mountain areas. *J. Hydrol.* **282** (1–4), 104–115. [https://doi.org/10.1016/S0022-1694\(03\)00257-9](https://doi.org/10.1016/S0022-1694(03)00257-9) (2003).
50. Masiokas, M. H. et al. Current state and recent changes of the cryosphere in the Andes. *Front. Earth Sci.* **8**, 99. <https://doi.org/10.3389/feart.2020.00099> (2020).
51. RGI Consortium Randolph Glacier Inventory. *Dataset Global Glacier Outlines Version 6*. <https://doi.org/10.7265/4m1f-gd79> (2017). NSIDC: National Snow and Ice Data Center.
52. Crippen, R. et al. NASADEM Global Elevation Model: Methods and Progress. The International Archives of the Photogrammetry, Remote Sensing and Spatial Information Sciences XLI-B4. (2016). <https://doi.org/10.5194/isprs-archives-XLI-B4-125-2016>
53. Hock, R., Jansson, P. & Braun, L. N. Modelling the response of Mountain Glacier discharge to climate warming. In: (eds Huber, U. M., Bugmann, H. K. M. & Reasoner, M. A.) *Global Change and Mountain Regions*. Advances in Global Change Research, vol 23. Springer, Dordrecht. https://doi.org/10.1007/1-4020-3508-X_25 (2005).

Acknowledgements

We acknowledge LabEx OSUG@2020 (Investissement d'Avenir, ANR10 LABX56). AC thanks the National Agency for Research and Development (ANID)/Scholarship Program/DOCTORADO BECAS CHILE/2019-72200174. RA was supported by the European Research Council (ERC) under the European Union's Horizon Framework research and innovation programme (grant agreement N°101115565; ICE3 project). The APC (Article Processing Charges) of this article were financed by AFD (Agence Française de Développement) and IRD within the framework of the CECC (Water Cycle and Climate Change) project (Andes section).

Author contributions

AC, TC, and AR were involved in the study design. AC wrote the model implementation and produced the figures, tables, and first draft of the manuscript. RA and NC contributed to the model implementation. AC performed the first level of analysis, which was improved by input from all authors. All authors contributed to the review and editing of the paper.

Declarations

Competing interests

The authors declare no competing interests.

Additional information

Supplementary Information The online version contains supplementary material available at <https://doi.org/10.1038/s41598-025-88069-2>.

Correspondence and requests for materials should be addressed to A.C.

Reprints and permissions information is available at www.nature.com/reprints.

Publisher's note Springer Nature remains neutral with regard to jurisdictional claims in published maps and institutional affiliations.

Open Access This article is licensed under a Creative Commons Attribution-NonCommercial-NoDerivatives 4.0 International License, which permits any non-commercial use, sharing, distribution and reproduction in any medium or format, as long as you give appropriate credit to the original author(s) and the source, provide a link to the Creative Commons licence, and indicate if you modified the licensed material. You do not have permission under this licence to share adapted material derived from this article or parts of it. The images or other third party material in this article are included in the article's Creative Commons licence, unless indicated otherwise in a credit line to the material. If material is not included in the article's Creative Commons licence and your intended use is not permitted by statutory regulation or exceeds the permitted use, you will need to obtain permission directly from the copyright holder. To view a copy of this licence, visit <http://creativecommons.org/licenses/by-nc-nd/4.0/>.

© The Author(s) 2025